Dynamical Instability of the *XY* Spiral State of Ferromagnetic Condensates

R. W. Cherng,[1] V. Gritsev,[1] D. M. Stamper-Kurn,[2,3] and E. Demler[1]

[1]*Physics Department, Harvard University, Cambridge, Massachusetts 02138, USA*
[2]*Department of Physics, University of California, Berkeley, California 94720, USA*
[3]*Materials Sciences Division, Lawrence Berkeley National Laboratory, Berkeley, California 94720, USA*

(Received 22 October 2007; revised manuscript received 9 January 2008; published 7 May 2008)

We calculate the spectrum of collective excitations of the *XY* spiral state prepared adiabatically or suddenly from a uniform ferromagnetic $F = 1$ condensate. For spiral wave vectors past a critical value, spin wave excitation energies become imaginary indicating a dynamical instability. We construct phase diagrams as functions of spiral wave vector and quadratic Zeeman energy.

DOI: 10.1103/PhysRevLett.100.180404 PACS numbers: 05.30.Jp, 03.75.Kk, 03.75.Mn, 67.90.+z

Spinor condensates of ultracold atoms [1–10] are the latest addition to many-body systems with multicomponent order parameters. The high symmetry of such systems manifests itself through the possibility of a variety of spin textures and topological defects. Although spin textures have been observed in liquid crystal nematics and superfluid ^{3}He, their nonequilibrium quantum dynamics are accessible in spinor condensates. Many open problems of quantum magnets and spinful superfluids, from the Kibble-Zurek mechanism of nucleating topological defects across a quantum phase transition [11] to fundamental limits of spinor Bose-Einstein condensation magnetometers [12] require understanding the dynamics of spin textures.

We investigate theoretically the stability of spin spirals in ferromagnetic $S = 1$ condensates (see Fig. 1). This simple spin structure can be prepared experimentally by applying a magnetic field gradient direction perpendicular to the magnetization axis [13]. A magnetic field gradient induces relative motion for different spin components which gives rise to a spiral magnetization with faster (slower) winding for stronger (weaker) gradients.

Our main result is the prediction of dynamical instabilities for spiral states, summarized in Fig. 2. Rotation of the magnetization vector from the *XY* plane to the z axis drives the instability at small quadratic Zeeman energy while rotations within the *XY* plane are responsible at large quadratic Zeeman energy. Surprisingly, we observe unstable modes can have wave vectors considerably larger than that of the initial spiral state. Previous works that have studied instabilities in spinor condensates include Castaing instabilities [14] in incoherent noncondensed two component ^{87}Rb [15] and the modulational instability of a uniform spinor condensate [16–18].

We analyze the mean-field and collective modes of the Gross-Pitaevskii equation derived from the Hamiltonian

$$\mathcal{H} = \mathbf{\Psi}^\dagger\left[-\frac{\nabla^2}{2m} - \mu - pF_z + qF_z^2\right]\mathbf{\Psi} + \frac{g_0}{2}:(\mathbf{\Psi}^\dagger\mathbf{\Psi})(\mathbf{\Psi}^\dagger\mathbf{\Psi}): + \frac{g_s}{2}:(\mathbf{\Psi}^\dagger\mathbf{\Psi}^*)(\mathbf{\Psi}^T\mathbf{\Psi}): \quad (1)$$

where $\mathbf{\Psi}_\alpha$ with $\alpha = x, y, z$ are annihilation operators for $F = 1$ bosons with mass m and $(F_\alpha)_{\beta\gamma}$ are angular momentum operators. We use a matrix notation with suppressed indices where $*$, T, and $\dagger$ denote the complex conjugate, transpose, and the conjugate transpose, respectively. For example, $\mathbf{\Psi}$ ($\mathbf{\Psi}^\dagger$) is a column (row) vector while F_z is a matrix.

Interaction strengths are given by $g_0 = 4\pi\hbar^2 a_0/m$, $g_s = 4\pi\hbar^2(a_0 - a_2)/3m$ [7] in terms of the s-wave scattering lengths a_F for two atoms colliding with total angular momentum F and $::$ denotes normal ordering. For ^{87}Rb, $a_0 = 101.8a_B$ and $a_2 = 100.4a_B$ where a_B is the Bohr radius [19] giving positive g_s and ferromagnetic interactions.

This Hamiltonian has a $U(1) \otimes SO(2)$ symmetry of global phase rotations and spin rotations about the z axis. The chemical potential μ and linear Zeeman energy p are Lagrange multipliers controlling the corresponding conserved quantities

$$\langle\mathbf{\Psi}^\dagger\mathbf{\Psi}\rangle = n, \qquad \langle\mathbf{\Psi}^\dagger F_z\mathbf{\Psi}\rangle = nf_z \quad (2)$$

where n is the total particle density and f_z is the z component of the magnetization per particle.

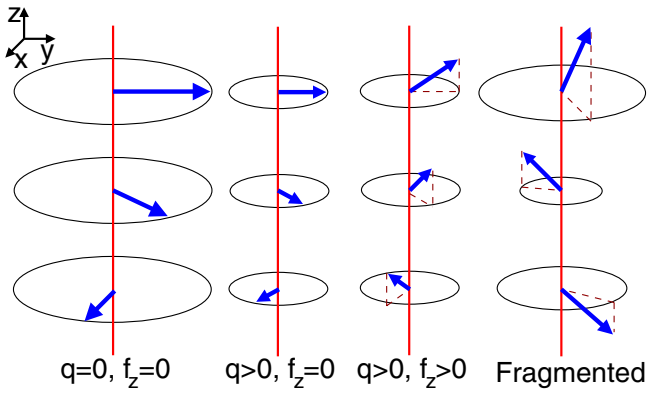

FIG. 1 (color online). From left to right: magnetization vector in the *XY* spiral state for fully polarized, partially polarized, $f_z \neq 0$, and after fragmentation.

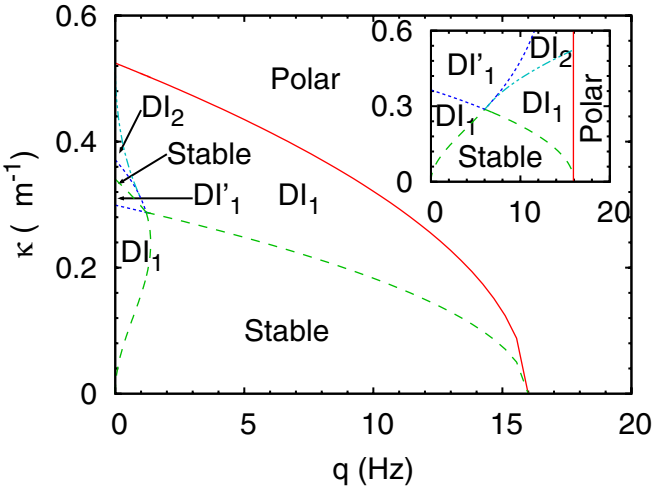

FIG. 2 (color online). Collective mode phase diagrams for $f_z = 0$ against spiral wave vector κ and quadratic Zeeman energy q in the adiabatic and sudden (inset) limits. DI_1 (DI_1') indicates a dynamical instability with one branch of unstable modes beginning at $k = 0$ ($k > 0$). DI_2 indicates a dynamical instability with two distinct branches of unstable modes.

Because of conservation of F_z, static magnetic fields enter through the quadratic Zeeman energy q instead of the linear Zeeman energy p. Moreover, q can be further manipulated through the ac Stark shifts. From here on, we take representative values $q = 70\ \mathrm{Hz\,G^{-2}}\ B^2$ where B is the magnetic field and $n = 2.2 \times 10^{14}\ \mathrm{cm}^{-3}$ [4]. We neglect here magnetic dipole interactions [20,21].

The XY spiral state is prepared from an initial cigar shaped condensate with uniform XY magnetization by applying a magnetic field gradient along the axial or z axis. After switching off the gradient, the transverse magnetization is imaged. It is fully polarized for $q = f_z = 0$ and is suppressed due to population of the $m_z = 0$ component of $\mathbf{\Psi}$ when $q \neq 0$ or $f_z \neq 0$. Fragmentation into domains carrying different magnetization vectors occurs when there is an instability.

Nonequilibrium *dynamics* governs the generation of the XY spiral state. We focus on studying the resulting nonequilibrium *stationary state* which we describe as a coherent condensate. They are mean-field solutions of the Gross-Pitaevskii (GP) equations implied by Eq. (1) which carry XY spiral order. In contrast to stable ground states, these nonequilibrium stationary states are in general metastable and decay via linear and nonlinear processes. We consider their linear stability by analyzing the spectrum of collective modes. The distinction between stable and metastable stationary states also arises for spinless bosons in a moving optical lattice [22,23] and four-wave mixing instabilities in optics such as the superradiance instability [24].

We perform a unitary transformation from the lab frame to a frame comoving with the XY spiral order. This is accomplished by the substitution

$$\mathbf{\Psi} \rightarrow \exp(i\kappa z F_z)\mathbf{\Psi}, \tag{3}$$

where κ is the spiral wave vector. Equation (1) with the substitution

$$p \rightarrow p + \frac{i\kappa}{m}\nabla_z, \qquad q \rightarrow q + \frac{\kappa^2}{2m} \tag{4}$$

gives the comoving frame Hamiltonian. After performing this transformation, we can do a similar analysis as in Ref. [25]. However, notice there is an important gaugelike term linear in the momentum. We use this unitary transformation as a formal step in the mathematical analysis, but we note continuous Raman excitation [26] may physically implement such a transformation.

We first focus on the adiabatic limit where the populations for components of $\mathbf{\Psi}$ can adjust to accommodate XY spiral order. This occurs via f_z conserving spin flip processes that mix the components of $\mathbf{\Psi}$. Gains in the interaction energy then offset the kinetic energy cost for the winding spiral. We note the adiabatic limit here refers to preparation of the spiral state on time scales slower than that of spin flips which occur in tens of milliseconds but faster than the trap oscillation frequencies which are of the order of hundreds of milliseconds for the long axis. For states prepared on slower time scales, Kohn oscillations [27] describing center of mass motion for different spin components could play a significant role for instabilities of the spiral state.

Uniform mean-field solutions in the comoving frame and a Cartesian basis are given by $\mathbf{\Psi} = \sqrt{n}\mathbf{\Phi}e^{i\omega t}$ with

$$\mathbf{\Phi} = \begin{bmatrix} ie^{i\eta + i\eta_\perp}\cos(\phi + i\chi)\sqrt{\frac{f_z}{\sinh(2\chi)}} \\ ie^{i\eta + i\eta_\perp}\sin(\phi + i\chi)\sqrt{\frac{f_z}{\sinh(2\chi)}} \\ e^{i\eta}\sqrt{1 - f_z\coth(2\chi)} \end{bmatrix}, \tag{5}$$

which give the conserved quantities of Eq. (3) by construction. It is instructive to also consider this mean-field solution in the lab frame using the $f_z = +1, 0, -1$ basis where $\mathbf{\Phi} \sim [e^{-i\kappa z}, 1, e^{+i\kappa z}]^T$. Notice each component of $\mathbf{\Phi}$ is an eigenstate of P_z the total momentum along z although $\mathbf{\Phi}$ as a vector is not. Moreover, the fluctuations of P_z given by $\langle \Delta P_z^2 \rangle = n\mathbf{\Phi}^\dagger \Delta P_z^2 \mathbf{\Phi}$ scales with the particle number.

Here η is a global phase that spontaneously breaks $U(1)$ phase rotation symmetry while ϕ gives the orientation of the magnetization vector in the XY plane and breaks $SO(2)$ spin rotation symmetry. $\eta_\perp$ is the relative phase between the z and transverse components and given by $\eta_\perp = \pi/2$ and $\eta_\perp = 0$ for antiferromagnetic and ferromagnetic interactions, respectively. χ controls the relative magnitude between the z and transverse components. The GP equations give

$$Q\tau^3 + (1 - Q)\tau = f_z, \tag{6}$$

where $\tau = \tanh(\chi)$ and $Q = q/2g_s n$. As in Ref. [25], we find three classes of polar, ferromagnet, and XY spiral state solutions. The polar (ferromagnet) state occurs for $f_z = 0$ and $Q > 1$ ($f_z = \pm 1$) and neither support XY spiral order.

Focusing first on the $f_z = 0$ case, we analyze next the spectrum of collective fluctuations $\delta\mathbf{\Phi}$ where $\mathbf{\Psi} = \sqrt{n}(\mathbf{\Phi} + \delta\mathbf{\Phi})e^{i\omega t}$. Bogoliubov analysis gives the excitation energies ω_k implicitly via the eigenvalue equation

$$0 = \det\begin{bmatrix} M_k - \omega_k & N \\ -N^* & -M_{-k}^* - \omega_k \end{bmatrix},$$
$$M_k = \frac{k^2}{2m} - \mu - \left(p + \frac{\kappa k_z}{m}\right)F_z + \left(q + \frac{\kappa^2}{2m}\right)F_z^2 + g_0 n\mathbf{\Phi}^\dagger\mathbf{\Phi} + g_0 n\mathbf{\Phi}\mathbf{\Phi}^\dagger + 2g_s n\mathbf{\Phi}^*\mathbf{\Phi}^T, \quad (7)$$
$$N = g_0 n\mathbf{\Phi}\mathbf{\Phi}^T + g_s n\mathbf{\Phi}^T\mathbf{\Phi},$$

in a matrix notation with $\mathbf{\Phi}^\dagger\mathbf{\Phi}$ ($\mathbf{\Phi}\mathbf{\Phi}^\dagger$) a scalar (matrix). We consider the one-dimensional case where $k_z = k$.

The XY spiral state spontaneously breaks $U(1) \otimes SO(2)$ symmetry of global phase and spin rotations giving a gapless charge and spin mode with linear dispersions. However, the spin mode can develop imaginary frequencies indicating a dynamical instability with several distinct types of behavior. The first is a branch of unstable modes starting at $k = 0$ denoted by DI_1 (Fig. 3). The second is a branch of unstable modes starting at $k > 0$ denoted by DI_1'. The third is two distinct branches of unstable modes starting at $k = 0$ and $k > 0$ denoted by DI_2 (inset Fig. 3).

We construct the phase diagrams of Fig. 2 as functions of the spiral wave vector κ and quadratic Zeeman energy q by characterizing the behavior of the spin mode. We first consider the adiabatic limit characterized by an interpolation between long-wavelength instabilities in the limit of large and small q. Both instabilities can be thought of as unwinding of the spiral order, but with qualitatively different origins.

When q is zero, the system is rotationally symmetric and the spiral state arbitrary $SO(3)$ rotations can unwind the magnetization vector from the XY plane to the z axis.

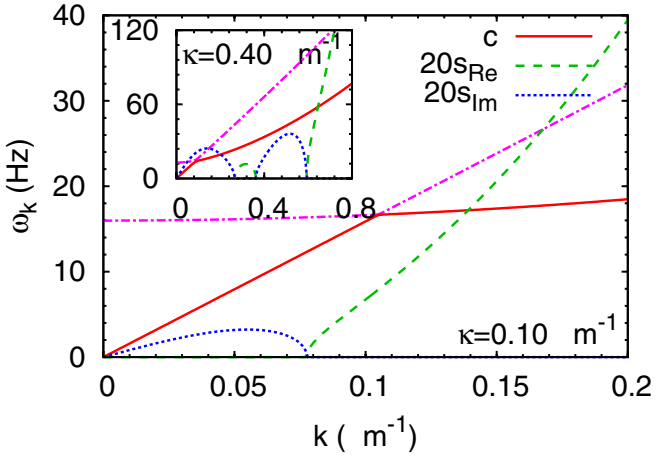

FIG. 3 (color online). Representative collective mode dispersions for $f_z = 0$ and $q = 0.2$ Hz in the adiabatic limit illustrating one (two) branches of unstable modes. c (s) denotes the charge (spin) mode.

Small q provides a potential energy barrier which can be overcome with sufficient kinetic energy stored in the nonuniform winding. Small fluctuations corresponding to such rotations can then grow exponentially giving rise to a dynamical instability. In particular, fluctuations in the *direction* of the magnetization vector drive the instability.

In contrast, large q explicitly breaks full $SO(3)$ rotational symmetry and confines rotations that unwind the spiral order to the XY plane. Such rotations proliferate near the quantum phase transition to the polar state when fluctuations in the *magnitude* of the magnetization vector are large.

This large q instability maps to the instability of current carrying states for spinless bosons [28]. Here the $SO(2)$ magnetization order parameter maps to the $U(1)$ order parameter of spinless bosons. The critical fluctuations near the transition to the polar state map to those of bosons near the Mott transition.

From the above arguments, we expect the XY spiral state to be stable for wave vectors less than $\kappa^2/2m \sim q$ or $\kappa^2/2m \sim (q - q_c)$ when q is small or large, respectively. Here q_c marks the transition point from the ferromagnet to the polar state in the uniform system. The boundaries in Fig. 2 can be obtained explicitly [29]

$$\frac{\kappa^2}{2m} \le \frac{2g_s n - q}{3 + 2\frac{g_s}{g_0}}, \qquad q \ge \frac{\kappa^2}{2m}\left(\frac{g_s n - \frac{\kappa^2}{2m}}{g_s n + \frac{\kappa^2}{2m}}\right), \quad (8)$$

which gives $\kappa^2/2m \le q$ and $\kappa^2/2m = (q_c - q)/3$ in agreement with the small and large q limits, respectively. We find the size of this region of instability scales with the strength of interactions $g_s n$ and vanishes in the limit of zero interactions.

Also notice in Fig. 2 an isolated line of stability at small q and intermediate κ. In the DI_1' region surrounding this line, the instability is weak with the imaginary part of ω_k relatively small. The energetic arguments at small q seem to suggest increasing κ makes the XY spiral state *more* unstable but this ignores the appreciable change in populations as κ continues to increase.

The spiral state in this limit has a significant polar component. It has been shown previously that the polar state has a dynamical instability with a characteristic wave vector $k \sim \sqrt{2mg_s n}$ [16]. When the spiral wave vector is on the order of this characteristic wave vector, the spiral order suppresses the instability of the polar component and the spiral state becomes *less* unstable.

After analyzing the $f_z = 0$ case in detail, we now briefly discuss the $f_z \neq 0$ case. The collective mode phase diagrams for the adiabatic limit are shown in the top of Fig. 4 with $f_z = 0.05$ to the left and $f_z = 0.5$ to the right. The small f_z phase diagrams are qualitatively similar to the $f_z = 0$ case. However, there is no polar state which only occurs for $f_z = 0$ but there is an additional region which exhibits a spin mode exhibiting a dispersion with negative frequencies describing a Landau instability. For large f_z,

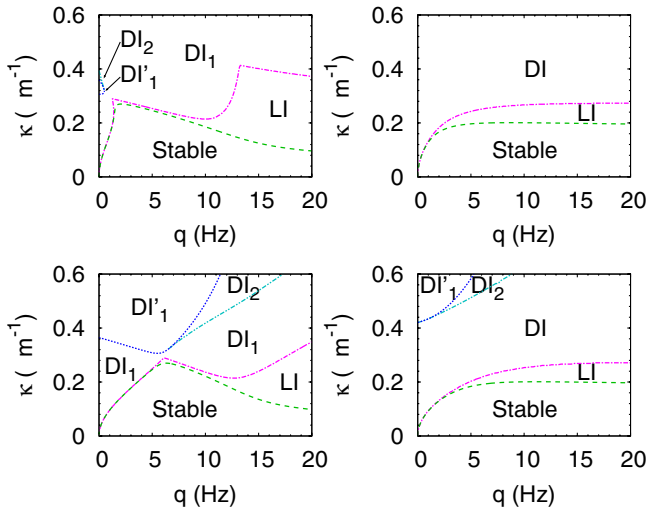

FIG. 4 (color online). Collective mode phase diagrams for $f_z = 0.05$ (left) and $f_z = 0.5$ (right) against spiral wave vector κ and quadratic Zeeman energy q in the adiabatic (top) and sudden (bottom) limits. DI (LI) indicates a dynamical (Landau) instability. DI_1, DI_1', and DI_2 are described in Fig. 2.

the phase diagrams no longer exhibit a characteristic peak for the stable region as a function of q.

So far the results have been focused on the adiabatic limit where the components of $\mathbf{\Psi}$ can adjust due to magnetization spin flip processes. In practice, the preparation of the XY spiral state can also occur on a time scale shorter than that of spin flips. We thus briefly comment on qualitatively similar results in the sudden limit where the populations of each component cannot change from their initial values. To take this effect into account, we consider mean-field solutions of the GP equation of the form $\mathbf{\Psi}_\alpha = \sqrt{n}\mathbf{\Phi}e^{i\omega_\alpha t}$ with $\omega_x = \omega_y \neq \omega_z$ and $\mathbf{\Phi}$ is as in Eq. (5). Notice the components of $\mathbf{\Psi}$ evolve at different frequencies, which allows for solutions with the necessary populations for each component.

We then perform the same analysis of the collective modes as in the adiabatic limit. This gives for $f_z = 0$ in the sudden limit the phase diagrams in the inset of Fig. 2. The origin of the instabilities in the sudden limit is the same and the region where the XY spiral state is stable is given by

$$\frac{\kappa^2}{2m} \leq \frac{2g_s n - q}{2 + 2\frac{g_s}{g_0}}, \qquad q \geq \frac{\kappa^2}{2m}\left(\frac{2g_s n}{g_s n + \frac{\kappa^2}{2m}}\right) \tag{9}$$

which gives $\kappa^2/2m = q/2$ and $\kappa^2/2m = (q_c - q)/2$ for the small q and large q limits, respectively. The $f_z = 0.05$ and $f_z = 0.5$ phase diagrams for the sudden limit are shown in the bottom of Fig. 4 and exhibit the same structure as the adiabatic limit.

In this Letter we have focused on the one-dimensional limit relevant for cigar shaped condensates. However, the formalism we used can be readily adapted for the three-dimensional case. In particular, one simply takes $k_z = k\cos\theta$ where θ is the angle between the mode wave vector and spiral wave vector in Eq. (7).

In summary, we studied a possible mechanism for the instability of the XY spiral state. Focusing on the limits where the XY spiral is prepared adiabatically or suddenly, we demonstrated that when the spiral wave vector exceeds a critical value spin wave energies become imaginary. This indicates the presence of a dynamical instability and exponential growth of fluctuations. We traced the physical origin of these instabilities to unwinding of the magnetization vector through rotations from the XY plane to the z axis for small quadratic Zeeman energy q and within the XY plane for large q.

This work was supported by NDSEG and the NSF Graduate Research Program, Harvard-MIT CUA, AFOSR, MURI, and the NSF Grant No. DMR-0132874. When this work was being completed we learned of the work by A. Lamacraft addressing related issues [30].

[1] J. Kronjäger *et al.*, Phys. Rev. A **72**, 063619 (2005).
[2] M.-S. Chang *et al.*, Nature Phys. **1**, 111 (2005).
[3] A. Widera *et al.*, New J. Phys. **8**, 152 (2006).
[4] L. E. Sadler *et al.*, Nature (London) **443**, 312 (2006).
[5] S. Foelling *et al.*, Nature (London) **448**, 1029 (2007).
[6] J. Stuhler *et al.*, Phys. Rev. Lett. **95**, 150406 (2005).
[7] T.-L. Ho, Phys. Rev. Lett. **81**, 742 (1998).
[8] T. Ohmi and K. Machida, J. Phys. Soc. Jpn. **67**, 1822 (1998).
[9] T.-L. Ho and S. K. Yip, Phys. Rev. Lett. **84**, 4031 (2000).
[10] M. Lewenstein *et al.*, Adv. Phys. **56**, 243 (2007).
[11] J. R. Anglin and W. H. Zurek, Phys. Rev. Lett. **83**, 1707 (1999).
[12] M. Vengalattore *et al.*, Phys. Rev. Lett. **98**, 200801 (2007).
[13] J. M. Higbie *et al.*, Phys. Rev. Lett. **95**, 050401 (2005).
[14] B. Castaing, Physica (Amsterdam) **126B**, 212 (1984).
[15] A. Kuklov and A. E. Meyerovich, Phys. Rev. A **66**, 023607 (2002).
[16] N. P. Robins *et al.*, Phys. Rev. A **64**, 021601 (2001).
[17] H. Saito and M. Ueda, Phys. Rev. A **72**, 023610 (2005).
[18] A. Lamacraft, Phys. Rev. Lett. **98**, 160404 (2007).
[19] E. G. M. van Kempen *et al.*, Phys. Rev. Lett. **88**, 093201 (2002).
[20] S. Yi *et al.*, Phys. Rev. Lett. **93**, 040403 (2004).
[21] Y. Kawaguchi *et al.*, Phys. Rev. Lett. **98**, 110406 (2007).
[22] B. Wu and Q. Niu, Phys. Rev. A **64**, 061603 (2001).
[23] A. Smerzi *et al.*, Phys. Rev. Lett. **89**, 170402 (2002).
[24] A. Hasegawa and W. F. Brinkman, IEEE J. Quantum Electron. **16**, 694 (1980).
[25] K. Murata *et al.*, Phys. Rev. A **75**, 013607 (2007).
[26] J. Higbie and D. M. Stamper-Kurn, Phys. Rev. Lett. **88**, 090401 (2002).
[27] C. J. Pethick and H. Smith, *Bose-Einstein Condensation in Dilute Gases* (Cambridge University Press, Cambridge, U.K., 2001).
[28] E. Altman *et al.*, Phys. Rev. Lett. **95**, 020402 (2005).
[29] R. W. Cherng *et al.* (to be published).
[30] A. Lamacraft, arXiv:0710.1848.